Published in final edited form as:
Genesis. 2009 July ; 47(7): 447–455. doi:10.1002/dvg.20522.

Transthyretin Mouse Transgenes Direct RFP Expression or Cre-Mediated Recombination Throughout the Visceral Endoderm

Gloria S. Kwon[1,2] and **Anna-Katerina Hadjantonakis**[1,*]

[1] Developmental Biology Program, Sloan-Kettering Institute, New York, New York

[2] Neuroscience Program, Weill Graduate School of Medical Sciences of Cornell University, New York, New York

Summary

Transthyretin (Ttr) is a thyroid hormone transport protein secreted by cells of the visceral yolk sac and fetal liver in developing embryos, and by hepatocytes and the choroid plexus epithelium of the brain in adult mice. Spatiotemporal localization of *Ttr* mRNA during embryogenesis suggested that *Ttr* regulatory elements might drive transgene expression throughout the visceral endoderm of early mouse embryos. We use *Ttr cis*-regulatory elements to generate *Ttr::RFP* and *Ttr::Cre* strains of mice, driving red fluorescent protein (RFP) and a nuclear-localized Cre recombinase, respectively. Visualization of RFP fluorescence in *Ttr::RFP* transgenics confirms reporter localization throughout the visceral endoderm in early embryos and in the visceral yolk sac and fetal liver of later stage embryos. Using both GFP-based and LacZ-based Cre reporter strains, we demonstrate that in *Ttr::Cre* transgenics, Cre-mediated recombination occurs throughout the visceral endoderm. The *Ttr::Cre* strain can therefore be used as a tool for genetic modifications within the visceral endoderm lineage.

Keywords

transgenic mice; transthyretin; visceral endoderm; fluorescent protein; RFP; Cre recombinase; Cre reporter; yolk sac; fetal liver; pancreas; stomach; intestine; limb

The visceral endoderm is an epithelium that overlies the extraembryonic ectoderm and epiblast of the early post-implantation mouse embryo. In addition to being involved in nutrient uptake and transport throughout embryogenesis, the visceral endoderm plays a critical role in the morphogenesis and patterning of the epiblast at early postimplantation stages (Beddington and Robertson, 1999; Lu *et al*., 2001; Srinivas, 2006; Tam and Loebel, 2007). The visceral endoderm is primarily fated to form the endoderm layer of the yolk sac, which expresses many secreted serum proteins in common with the fetal liver and adult hepatocytes (Costa *et al*., 1990; Meehan *et al*., 1984; Soprano *et al*., 1986).

Currently, there are only a limited number of *cis*-regulatory elements that have been shown to drive transgene activity specifically within the visceral endoderm. Transgenic strains such as *Hex::GFP* and *Cerl::GFP* label a sub-population of the visceral endoderm, comprising the anterior visceral endoderm (Mesnard *et al*., 2004; Rodriguez *et al*., 2001; Srinivas *et al*., 2004). We have previously demonstrated that Alpha-fetoprotein (Afp) regulatory elements drive transgenene expression throughout the visceral endoderm and that *Afp::GFP* transgenics

*Correspondence to: Anna-Katerina Hadjantonakis, Developmental Biology Program, Sloan-Kettering Institute, New York, NY 10065, USA. hadj@mskcc.org.

represent the first pan-visceral endoderm reporter strain (Kwon *et al*., 2006). However, in early post-implantation stage (pre- to mid-streak stages) *Afp::GFP* embryos, GFP fluorescence is specifically localized throughout the visceral endoderm in the distal half of the conceptus overlying the epiblast, but absent in more proximal visceral endoderm overlying the extraembryonic ectoderm (Kwon *et al*., 2006). This is due to repression of *Afp* by signals from the extraembryonic ectoderm (Dziadek, 1978), which is relieved at later (mid to late streak) stages coincident with the formation of extraembryonic mesoderm (Dziadek, 1978; Dziadek and Adamson, 1978). Based on these observations, we wanted to identify alternative *cis*-regulatory elements that would drive transgene expression throughout the visceral endoderm lineage in early postimplantation embryos.

Transthyretin (Ttr) is a thyroid hormone transport protein secreted by hepatocytes and the choroid plexus epithelium of adult mice, and by cells of the visceral yolk sac of developing embryos (Costa *et al*., 1990; Yan *et al*., 1990). Since *Ttr* mRNA expression assayed by in situ hybridization had been shown to localize to the entire visceral endoderm at pre-streak (PS) stages (Mesnard *et al*., 2006), we reasoned that *cis*-regulatory elements from the *Ttr* locus would be good candidates for driving transgene expression throughout the visceral endoderm. To evaluate the *Ttr cis*-regulatory elements, we generated strains of mice that were used to direct fluorescent protein reporter expression. Having previously demonstrated robust widespread expression and developmental neutrality of mRFP1 in mouse embryonic stem (ES) cells and embryos (Long *et al*., 2005) and wanting to provide a spectrally distinct reporter from the existing *Afp::GFP* (Kwon *et al*., 2006), we generated *Ttr::RFP* transgenic mice. A *Ttr* minigene consisting of a 3-kb upstream regulatory region, the first exon and intron, and a partial second exon (Yan *et al*., 1990) was used to drive the expression of monomeric red fluorescent protein (mRFP1) (Campbell *et al*., 2002). We observed RFP fluorescence throughout and specific to the visceral endoderm in early postimplantation embryos, and later in the yolk sac endoderm of *Ttr::RFP* transgenics.

A strain of mice exhibiting pan-visceral endoderm expression of *Cre* recombinase, which allows for site-specific DNA recombination and tissue-specific gene inactivation (Lewandoski, 2001), would provide a useful tool to study gene function within the visceral endoderm during embryonic development. Previous studies have, for example, used gene targeting at the *hepatocyte nuclear factor 4* (*Hnf4α*) locus to drive *Cre* recombinase expression in the visceral endoderm and various endoderm derivatives of the mouse embryo (Vincent and Robertson, 2004). However, despite the early onset of *Hnf4α* expression in the primitive endoderm in preimplantation stage embryos and maintenance of expression throughout the visceral endoderm at postimplantation stages (Duncan *et al*., 1994), *Cre* expression was detected in only a few cells within the visceral endoderm and not throughout the entire lineage in $Hnf4\alpha^{Cre}$ embryos (Vincent and Robertson, 2004). To produce a tool facilitating genetic modifications within the visceral endoderm, we generated *Ttr::Cre* transgenic mice. Our observations suggest that this strain drives Cre-mediated recombination throughout the visceral endoderm, and later in the yolk sac endoderm as well as in various endoderm-derived organs.

Ttr-RFP$^+$ CELLS IN POSTIMPLANTATION EMBRYOS

Ttr transcripts are expressed within the visceral endoderm in PS stage (E5.5) embryos (Fig. 1a), and remain specific to the visceral endoderm at later postimplantation stages (Fig. 1b,c). By midgestation (E9.5), *Ttr* transcripts are detected in the visceral yolk sac (Fig. 1d).

Two strains of *Ttr::RFP* transgenic mice were generated by inserting a 1-kb mRFP1 (Campbell *et al*., 2002) fragment into either the first (ex1) or second (ex2) exon of the *Ttr* minigene (Costa *et al*., 1990) (Fig. 1e). No detectable differences were observed in the spatial or temporal localization of RFP expression between the two transgenic strains. Ttr-RFP$^+$ cells were not

detected at peri-implantation stages (E4.5) (Fig. 1f). The onset of RFP fluorescence was first observed in blastocyst outgrowths 12 h after plating in a small cohort of cells (Fig. 1g). After 24–48 h of culture, the number of Ttr-RFP^{+} cells, as well as the intensity of RFP fluorescence was gradually increased (Fig. 1h,i).

In the early postimplantation embryo, RFP fluorescence was initiated at the PS stage (E5.5) specifically in the visceral endoderm (Fig. 1j). At the mid-streak (MS) stage (E6.5), RFP fluorescence was maintained in both the proximal and distal visceral endoderm (Fig. 1k). In double transgenic *Ttr::RFP*$^{Tg/+}$*; Afp::GFP*$^{Tg/+}$ embryos, RFP fluorescence was detected throughout the visceral endoderm, while GFP fluorescence was restricted to the distal visceral endoderm overlying the epiblast at the PS (E5.25) stage (Fig. 1l). By the MS (E6.5) stage, GFP fluorescence was gradually expanded into the proximal visceral endoderm (Fig. 1m). Of note, the levels of RFP fluorescence was reduced in comparison to GFP fluorescence at all stages examined in *Ttr::RFP*$^{Tg/+}$*; Afp::GFP*$^{Tg/+}$ double transgenics.

By the early to late bud (EB-LB) stages (E7.5), RFP was detected in the visceral endoderm overlying the extraembryonic ectoderm and a population of dispersed visceral endoderm-derived cells overlying the epiblast (Fig. 1n). By the 4–6 somite stage, RFP was restricted to the extra-embryonic visceral endoderm, while no fluorescence was detected in the region overlying the epiblast (Fig. 1o,p). The absence of RFP fluorescence distally in the region overlying the epiblast differs from our previous observations using *Afp::GFP* transgenics (Kwon *et al*., 2008), in which we demonstrated that the visceral endoderm does not become displaced proximally to extramembryonic regions as widely believed, but rather, that the visceral endoderm becomes dispersed in the region overlying the epiblast by widespread intercalation of epiblast-derived cells. We established that in *Afp::GFP* transgenics, fluorescence within this scattered population of cells overlying the epiblast was due to perdurance of GFP protein, as *GFP* mRNA was not present in this region (Kwon *et al*., 2008). We therefore attribute the differences in the levels of the fluorescent reporters observed between the *Afp::GFP* and *Ttr::RFP* strains to *Afp cis*-regulatory elements driving higher levels of transgene expression compared to *Ttr cis*-regulatory elements, resulting in greater perdurance of fluorescent protein in *Afp::GFP* transgenics. By midgestation, RFP fluorescence was restricted to the visceral yolk sac (Fig. 1q).

Cre EXPRESSION AND ACTIVITY IN EARLY POSTIMPLANTATION EMBRYOS

Having established that *Ttr cis*-regulatory elements drive pan-visceral endoderm reporter expression, we generated an additional transgenic strain *Ttr::Cre* by inserting a 1.1 kb *nls*Cre (Lewandoski *et al*., 1997) fragment into the second exon (ex2) of the *Ttr* minigene (Costa *et al*., 1990) (Fig. 2a). Wholemount in situ hybridization to detect *Cre* mRNA revealed pan-visceral endoderm *Cre* expression at PS stages (Fig. 2b). However by the MS-ESom (early somite, E8.5) stages, *Cre* mRNA was significantly reduced and was sparsely detected only in visceral endoderm overlying extraembryonic regions (Fig. 2c–e).

To evaluate Cre recombinase-mediated excision, we used both GFP-based and LacZ-based Cre reporter strains (Novak *et al*., 2000; Soriano, 1999). No Cre reporter activity was observed in double transgenic *Ttr::Cre*$^{Tg/+}$*; Z/EG*$^{Tg/+}$ or *Ttr::Cre*$^{Tg/+}$*; R26::LNL::LacZ*$^{+/-}$ at any stage of preimplantation development. At PS-MS stages, both the proximal and distal visceral endoderm was labeled with GFP in *Ttr::Cre*$^{Tg/+}$*; Z/EG*$^{Tg/+}$ embryos (Fig. 2f,g) in agreement with *Ttr::RFP* transgenics. By the LB-ESom stages, the Cre reporter was observed in the extraembryonic visceral endoderm and the population of scattered visceral endoderm-derived cells overlying the epiblast (Fig. 2h,i). Since *Cre* mRNA is largely downregulated in MS-ESom stage *Ttr::Cre*$^{Tg/+}$ embryos, we suggest that Cre reporter-activity results from excision at early postimplantation (PS-ES) stages.

Cre REPORTER ACTIVITY IN YOLK SAC ENDODERM

By midgestation (E9.5), both GFP and LacZ Cre reporter activity were detected within the endoderm of the visceral yolk sac (Fig. 3a,e), which persisted through to later gestational stages (E12.5 to E18.5) (Fig. 3b–d, f–h). Both *Ttr::Cre*$^{Tg/+}$*; R26::LNL::LacZ*$^{+/-}$ and *Ttr::Cre*$^{Tg/+}$*; Z/EG*$^{Tg/+}$ embryos exhibited some mosaic reporter activity within the yolk sac endoderm (Fig. 3b, e–g), which could be attributed to the mosaic reporter activity observed in the visceral endoderm directly adjacent to the ectoplacental cone in early postimplantation embryos (Figs. 1j,k and 2f,g). In *Ttr::Cre*$^{Tg/+}$*; R26::LNL::LacZ*$^{+/-}$ embryos, Cre reporter expression was detected in the liver at E12.5 and E15.5 (white arrowheads, Fig. 3b,c). GFP fluorescence was not detected in the liver in wholemount *Ttr::Cre*$^{Tg/+}$*; Z/EG*$^{Tg/+}$ embryos (Fig. 3f,g) due to low fluorescence intensity; however, transverse sections through E12.5 and E15.5 stage embryos revealed a mosaic GFP expressing population of cells within the fetal liver (data not shown).

High resolution confocal imaging and three-dimensional (3D) reconstructions of yolk sac, counterstained with Hoechst to label nuclei (red staining), from an E12.5 *Ttr::Cre*$^{Tg/+}$*; Z/EG*$^{Tg/+}$ embryo revealed GFP fluorescence restricted to the endoderm (Fig. 3i-i″). Transverse sections through the yolk sac of an E12.5 *Ttr::Cre*$^{Tg/+}$*; R26::LNL::LacZ*$^{+/-}$ embryo confirmed this observation (Fig. 3j).

Cre REPORTER ACTIVITY IN LATER ENDODERM DERIVATIVES

To analyze Cre reporter activity in later endoderm-derived tissues, we dissected organs of *Ttr::Cre*$^{Tg/+}$*; R26::LNL::LacZ*$^{+/-}$ embryos between E12.5 and E16.5, and visualized for β-gal activity. In all double transgenic embryos examined, Cre reporter activity was detected in organs containing endodermal derivatives such as the liver (Fig. 4a–c), pancreas (Fig. 4d–f), stomach (Fig. 4g–i), and intestine (Fig. 4j–l). Transverse sections through the liver at E12.5 revealed mosaic β-gal activity (Fig. 4a′), which gradually decreased at E14.5 (Fig. 4b′) and resulted in more uniform β-gal expression at E16.5 (Fig. 4c′). In the pancreas, β-gal activity was restricted to the pancreatic epithelium and excluded from the pancreatic mesenchyme at E12.5 and E14.5 (Fig. 4d′,e′) and by E16.5, Cre reporter activity was detected in cells likely representing the endocrine progenitor population (Fig. 4f′). The epithelial lining of the stomach and intestine both exhibited mosaic β-gal activity at E12.5 (Fig. 4g′,h′) and E14.5 (Fig. 4j′,k′), with higher levels of β-gal expression in more differentiated compartments of the stomach and gut epithelium by E16.5 (Fig. 4i′,l′). In all these organs, the gradual increase in the number of cells with β-gal expression could be attributed either to de novo activation of the transgene, and/or to proliferation of β-gal expressing cells that had previously undergone *Cre*-mediated excision. The development of *Ttr* transgenic strains expressing regulatable forms of the Cre recombinase should resolve this question.

ADDITIONAL SITES OF RFP EXPRESSION AND Cre RECOMBINATION IN LATE STAGE EMBRYOS

Approximately 10% of *Ttr::Cre*$^{Tg/+}$*; R26::LNL::LacZ*$^{+/-}$ transgenic embryos exhibited β-gal activity in additional sites, which was observed regardless of genetic background. These corresponded with sites of RFP fluorescence observed in all *Ttr::RFP* transgenics. Therefore, these additional sites of *Cre* recombinase activity represent an inherent feature of the *Ttr cis*-regulatory elements that is activated in a subset of *Ttr::Cre* transgenic embryos observed using both *Z/EG* and *R26::LNL::LacZ* Cre reporter strains.

Comparative analysis of the two transgenic strains at E12.5 revealed various overlapping regions of Cre reporter activity and RFP fluorescence (gray arrowheads, Fig. 5a-a′). In the craniofacial region, *Cre* recombinase activity correlated with RFP fluorescence in the optic

vesicle and diffusely throughout the hindbrain (Fig. 5b-b′) however, while reporter activity was detected in the frontal nasal process of *Ttr::Cre*$^{Tg/+}$*; R26::LNL::LacZ*$^{+/-}$ embryos (red arrowhead, Fig. 5a), no expression in this region was observed in *Ttr::RFP* transgenics. In *Ttr::Cre*$^{Tg/+}$*; R26::LNL::LacZ*$^{+/-}$ embryos, β-gal activity was detected in the neocortex and faintly in the midbrain–hindbrain boundary (Fig. 5c), while in *Ttr::RFP* embryos, RFP fluorescence was strongly expressed at the midbrain–hindbrain junction (blue arrowhead, Fig. 5a′), but only weakly detected in the neocortex (Fig. 5c′). In the limbs, mesenchymal condensations were labeled by both Cre reporter activity and RFP fluorescence (Fig. 5d-d′), but only *Ttr::Cre*$^{Tg/+}$*; R26::LNL::LacZ*$^{+/-}$ embryos exhibited reporter activity in the apical ectodermal ridge (AER) (black arrowheads, Fig. 5d), which was not observed in wild type control embryos (high magnification inset, Fig. 5d). Since we did not detect significant levels of endogenous β-gal activity in control embryos, we attribute the differences in expression patterns between *Ttr::Cre*$^{Tg/+}$*; R26::LNL::LacZ*$^{+/-}$ and *Ttr::RFP* transgenics to the additive nature of *Cre*-mediated recombination, which results in permanent labeling of cells and their progeny, while the fluorescent reporter only acts as a short-term label.

Both *Ttr::Cre*$^{Tg/+}$*; R26::LNL::LacZ*$^{+/-}$ and *Ttr::RFP* transgenic embryos exhibited reporter activity in several visceral organs dissected at E12.5. Cre reporter activity and RFP fluorescence were mosaic in the liver (Fig. 5e-e′) as well as in the epithelium of the stomach and intestine (Fig. 5g,h′), and were observed in the pancreatic endoderm but not in the pancreatic mesoderm (Fig. 5f-f′). The frequency of reporter activity in additional sites, likely due to de novo transgene activation, precludes further analysis of visceral endoderm-derived cells within embryonic endoderm derivatives. Future studies incorporating the *Ttr cis*-regulatory elements in a genetic inducible fate mapping approach should address the fate of cells originating in the visceral endoderm (Joyner and Zervas, 2006).

In summary, we have demonstrated that *Ttr cis*-regulatory elements drive pan-visceral endoderm transgene expression. *Ttr::RFP* and *Ttr::Cre* transgenic strains are useful tools for live imaging, fate mapping and genetically modifying cells of the visceral endoderm, the yolk sac endoderm, and several endoderm-derived organs including the fetal liver, pancreas, stomach, and intestine. Indeed, by directing pan-visceral endoderm-specific recombination, *Ttr::Cre* can be used in parallel with epiblast-specific Cre deleter strains, such as the *Sox2::Cre* and *MORE::Cre strains* (Hayashi *et al*., 2002; Tallquist and Soriano, 2000), to dissect gene function in the different cell layers of the early postimplantation mouse embryo.

METHODS

Transgene Construction and Strains Used

The *Ttr::RFP* constructs were generated by inserting a 1-kb mRFP1 (Campbell *et al*., 2002) fragment into either the *NruI* site of the first exon or *StuI* site of the second exon of *pTTR1ExV3* (Costa *et al*., 1990). The *Ttr::Cre* construct was generated by inserting a 1.1 kb *nls*Cre (Lewandoski *et al*., 1997) fragment into the second exon of *pTTR1ExV3* (Costa *et al*., 1990). Constructs were injected into (C57BL/6J X CBA/J)F1 mice and outbred onto ICR for five generations. Before backcrossing onto ICR, *Ttr::Cre* transgenic mice exhibited some degree of variability in *Cre*-mediated excision, which periodically included mosaic excision in the visceral endoderm and in epiblast derivatives. Other mouse strains used were: *ROSA26::LNL::LacZ* (B6.129S4-*Gt*(ROSA)26Sor^{tm1Sor}/J; JAX #3474) (Soriano, 1999), a LacZ-based Cre reporter, and Z/EG (B6.Cg-Tg(ACTB-Bgeo/GFP)21Lbe/J; JAX #3920), a GFP-based Cre reporter (Novak *et al*., 2000).

Embryo Collection

Preimplantation embryos were recovered in M2 medium and cultured in KSOM (Chemicon Specialty Media, Temecula, CA). For outgrowths, blastocysts were plated onto chambered coverglass (Lab-Tek II, Nunc, Rochester, NY) and cultured in ES-DMEM (Nagy *et al*., 2003) containing LIF for 12–48 h. Early postimplantation embryos were dissected in either PB-1 media (Papaioannou and West, 1981; Whittingham and Wales, 1969) containing 10% newborn calf serum or DMEM-F12 containing 5% newborn calf serum. Embryos were staged according to Downs and Davies (1993). Mid- to late-gestational stage embryos (E9.5–E18.5) were dissected in PBS containing 1% BSA and prepared for processing.

In Situ Hybridization and X-Gal Staining

Wholemount in situ hybridizations were performed according to standard protocols (Nagy *et al*., 2003). Anti-sense riboprobes used were Ttr (Wakasugi *et al*., 1985), Cre, and RFP. To detect Cre and RFP transcripts, anti-sense probes were generated by subcloning either a Cre (Lewandoski *et al*., 1997) or mRFP1 (Campbell *et al*., 2002) fragment into pBluescript SK+. For wholemount LacZ staining, embryos were fixed in 0.2% glutaraldehyde solution for 20 min to 1 h, followed by washes in phosphate detergent rinse (0.1 M sodium phosphate, 2 mM $MgCl_2$, 0.01% sodium deoxycholate, 0.02% NP-40) and staining in X-gal staining solution (phosphate detergent rinse containing 5 mM $K_3[Fe(CN)_6]$, 5 mM $K_4(Fe(CN)_6]$, and 1 mg/ml X-gal) to detect β galactosidase activity (Nagy *et al*., 2003). For LacZ staining of internal organs, embryos were fixed in 0.2% glutaraldehyde, processed for cryosectioning, and sectioned at 20–30 μm. Sections were washed and then stained in X-gal staining solution.

Immunohistochemistry

Embryos were blocked for 1 h at RT in PBSMT, and then incubated with either anti-RFP (1:500; Abcam, Cambridge, MA) or anti-GFP (1:500, Molecular Probes, Eugene, OR) antibodies. The next day, embryos were washed with PBSMT and incubated with Vectastain blocking solution (Vector Labs, Burlingame, CA) for 1 h at RT, followed by incubation with a biotinylated secondary antibody at 4° overnight. Embryos were then washed with PBSMT and rinsed in PBT before being incubated with Streptavidin-AlexaFluor546 or Streptavidin-AlexaFluor488 (Molecular Probes) for 1 h at RT in the dark. Finally, embryos were washed in PBT and imaged. Yolk sacs were counterstained with Hoechst to detect nuclei (Invitrogen, Carlsbad, CA).

Image Acquisition and Processing

Widefield images were acquired using a Zeiss Axiocam MRc or MRm CCD camera mounted on a Leica MZ16FA microscope. Laser scanning confocal data were acquired using a Zeiss LSM 510 META mounted on a Zeiss Axiovert 200M microscope. Fluorophores were excited using either a 405-nm diode laser (Hoechst), 488-nm argon laser (Alexa488 and GFP), or 543-nm HeNe laser (Alexa546 and RFP). Objectives used were plan-achromat 20x/NA0.75 and fluar 5x/NA0.25. For live imaging experiments, embryos were imaged wholemount in Mat-Tek (Ashland, MA) glass bottom dishes and kept in a humidified, temperature-controlled chamber with 5% CO_2 atmosphere. Sections were mounted onto slides and imaged through glass coverslips. Raw data were processed using Zeiss AIM software (Carl Zeiss Microsystems, http://www.zeiss.com/). Figures were assembled in Adobe Photoshop CS2.

Acknowledgments

Contract grant sponsor: National Institutes of Health, Contract grant number: RO1-HD052115

The authors thank the Memorial Sloan-Kettering Cancer Center Mouse Genetics Core Facility for production of transgenic strains; Terry Van Dyke for the *Ttr cis*-regulatory elements; Roger Tsien for the mRFP1 plasmid; Mark Lewandoski for the *nls*Cre plasmid; Liz Lacy and Sonja Nowotschin for comments on the manuscript.

LITERATURE CITED

Beddington RS, Robertson EJ. Axis development and early asymmetry in mammals. Cell 1999;96:195–209. [PubMed: 9988215]

Campbell RE, Tour O, Palmer AE, Steinbach PA, Baird GS, Zacharias DA, Tsien RY. A monomeric red fluorescent protein. Proc Natl Acad Sci USA 2002;99:7877–7882. [PubMed: 12060735]

Costa RH, Van Dyke TA, Yan C, Kuo F, Darnell JE Jr. Similarities in transthyretin gene expression and differences in transcription factors: Liver and yolk sac compared to choroid plexus. Proc Natl Acad Sci USA 1990;87:6589–6593. [PubMed: 2395861]

Downs KM, Davies T. Staging of gastrulating mouse embryos by morphological landmarks in the dissecting microscope. Development 1993;118:1255–1266. [PubMed: 8269852]

Duncan SA, Manova K, Chen WS, Hoodless P, Weinstein DC, Bachvarova RF, Darnell JE Jr. Expression of transcription factor HNF-4 in the extraembryonic endoderm, gut, and nephrogenic tissue of the developing mouse embryo: HNF-4 is a marker for primary endoderm in the implanting blastocyst. Proc Natl Acad Sci USA 1994;91:7598–7602. [PubMed: 8052626]

Dziadek M. Modulation of alphafetoprotein synthesis in the early postimplantation mouse embryo. J Embryol Exp Morphol 1978;46:135–146. [PubMed: 81255]

Dziadek M, Adamson E. Localization and synthesis of alphafoeto-protein in post-implantation mouse embryos. J Embryol Exp Morphol 1978;43:289–313. [PubMed: 75937]

Hayashi S, Lewis P, Pevny L, McMahon AP. Efficient gene modulation in mouse epiblast using a Sox2Cre transgenic mouse strain. Mech Dev 2002;119 (Suppl 1):S97–S101. [PubMed: 14516668]

Joyner AL, Zervas M. Genetic inducible fate mapping in mouse: Establishing genetic lineages and defining genetic neuroanatomy in the nervous system. Dev Dyn 2006;235:2376–2385. [PubMed: 16871622]

Kwon GS, Fraser ST, Eakin GS, Mangano M, Isern J, Sahr KE, Hadjantonakis AK, Baron MH. Tg(Afp-GFP) expression marks primitive and definitive endoderm lineages during mouse development. Dev Dyn 2006;235:2549–2558. [PubMed: 16708394]

Kwon GS, Viotti M, Hadjantonakis AK. The endoderm of the mouse embryo arises by dynamic widespread intercalation of embryonic and extraembryonic lineages. Dev Cell 2008;15:509–520. [PubMed: 18854136]

Lewandoski M. Conditional control of gene expression in the mouse. Nat Rev Genet 2001;2:743–755. [PubMed: 11584291]

Lewandoski M, Wassarman KM, Martin GR. Zp3-cre, a transgenic mouse line for the activation or inactivation of loxP-flanked target genes specifically in the female germ line. Curr Biol 1997;7:148–151. [PubMed: 9016703]

Long JZ, Lackan CS, Hadjantonakis AK. Genetic and spectrally distinct in vivo imaging: Embryonic stem cells and mice with widespread expression of a monomeric red fluorescent protein. BMC Biotechnol 2005;5:20. [PubMed: 15996270]

Lu CC, Brennan J, Robertson EJ. From fertilization to gastrulation: Axis formation in the mouse embryo. Curr Opin Genet Dev 2001;11:384–392. [PubMed: 11448624]

Meehan RR, Barlow DP, Hill RE, Hogan BL, Hastie ND. Pattern of serum protein gene expression in mouse visceral yolk sac and foetal liver. EMBO J 1984;3:1881–1885. [PubMed: 6479150]

Mesnard D, Filipe M, Belo JA, Zernicka-Goetz M. The anterior-posterior axis emerges respecting the morphology of the mouse embryo that changes and aligns with the uterus before gastrulation. Curr Biol 2004;14:184–196. [PubMed: 14761650]

Mesnard D, Guzman-Ayala M, Constam DB. Nodal specifies embryonic visceral endoderm and sustains pluripotent cells in the epiblast before overt axial patterning. Development 2006;133:2497–2505. [PubMed: 16728477]

Nagy, A.; Gertsenstein, M.; Vintersten, K.; Behringer, R. Manipulating the mouse embryo: A laboratory manual. Cold Spring Harbor, New York: Cold Spring Harbor Laboratory Press; 2003.

Novak A, Guo C, Yang W, Nagy A, Lobe CG. Z/EG, a double reporter mouse line that expresses enhanced green fluorescent protein upon Cre-mediated excision. Genesis 2000;28:147–155. [PubMed: 11105057]

Papaioannou VE, West JD. Relationship between the parental origin of the X chromosomes, embryonic cell lineage and X chromosome expression in mice. Genet Res 1981;37:183–197. [PubMed: 7262553]

Rodriguez TA, Casey ES, Harland RM, Smith JC, Beddington RS. Distinct enhancer elements control Hex expression during gastrulation and early organogenesis. Dev Biol 2001;234:304–316. [PubMed: 11397001]

Soprano DR, Soprano KJ, Goodman DS. Retinol-binding protein and transthyretin mRNA levels in visceral yolk sac and liver during fetal development in the rat. Proc Natl Acad Sci USA 1986;83:7330–7334. [PubMed: 3463972]

Soriano P. Generalized lacZ expression with the ROSA26 Cre reporter strain. Nat Genet 1999;21:70–71. [PubMed: 9916792]

Srinivas S. The anterior visceral endoderm-turning heads. Genesis 2006;44:565–572. [PubMed: 17078044]

Srinivas S, Rodriguez T, Clements M, Smith JC, Beddington RS. Active cell migration drives the unilateral movements of the anterior visceral endoderm. Development 2004;131:1157–1164. [PubMed: 14973277]

Tallquist MD, Soriano P. Epiblast-restricted Cre expression in MORE mice: A tool to distinguish embryonic vs. extra-embryonic gene function. Genesis 2000;26:113–115. [PubMed: 10686601]

Tam PP, Loebel DA. Gene function in mouse embryogenesis: Get set for gastrulation. Nat Rev Genet 2007;8:368–381. [PubMed: 17387317]

Vincent SD, Robertson EJ. Targeted insertion of an IRES Cre into the Hnf4α locus: Cre-mediated recombination in the liver, kidney, and gut epithelium. Genesis 2004;39:206–211. [PubMed: 15282747]

Wakasugi S, Maeda S, Shimada K, Nakashima H, Migita S. Structural comparisons between mouse and human prealbumin. J Biochem 1985;98:1707–1714. [PubMed: 3005251]

Whittingham DG, Wales RG. Storage of two-cell mouse embryos in vitro. Aust J Biol Sci 1969;22:1065–1068. [PubMed: 5374532]

Yan C, Costa RH, Darnell JE Jr, Chen JD, Van Dyke TA. Distinct positive and negative elements control the limited hepatocyte and choroid plexus expression of transthyretin in transgenic mice. EMBO J 1990;9:869–878. [PubMed: 1690125]

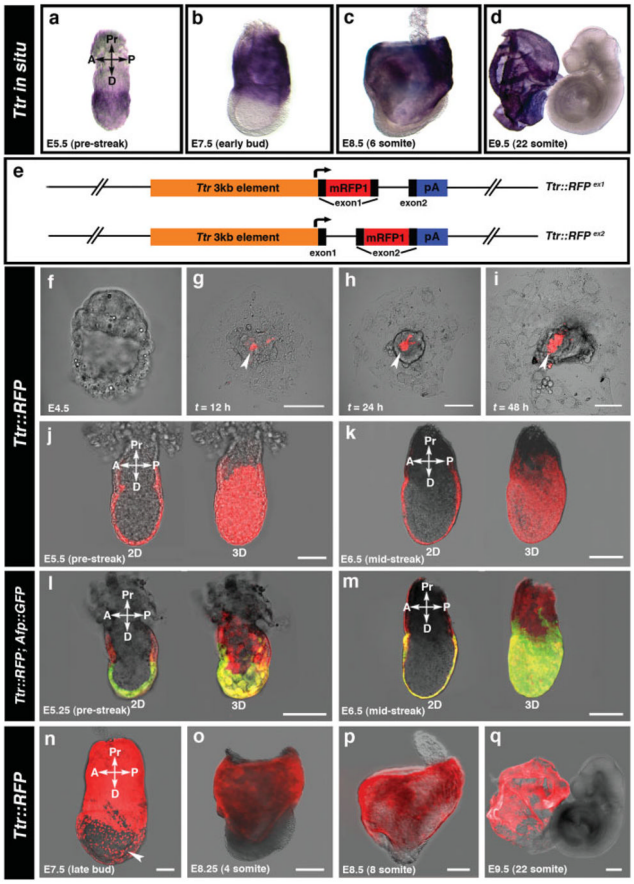

FIG. 1.

Regulatory elements from the *Ttr* locus drive transgene activity throughout the visceral endoderm. (**a–d**) *Ttr* mRNA in situ hybridization in prestreak (E5.5) through to 22 somite stage (E9.5) embryos. (**e**) Schematic representation of the two different *Ttr::RFP* transgenes. mRFP1 inserted into the first exon (top); alternate version with mRFP1 insertion into the second exon (bottom). (**f**) Absence of RFP fluorescence in peri-implantation stage (E4.5) $Ttr::RFP^{Tg/+}$ embryos. (**g–i**) Onset of RFP fluorescence is detected in blastocyst outgrowths as a small cohort of cells 12 h after plating (g) and is gradually expressed in more cells after 24 h (h) and 48 h (i). (**j,k**) $Ttr::RFP^{Tg/+}$ embryos exhibit RFP fluorescence specifically throughout the visceral endoderm at PS (E5.5) (j) and MS (E6.5) stages (k) shown as 2D optical sections (left) and 3D reconstructions of confocal *z*-stacks (right). (**l,m**) At PS (E5.25) stages, double transgenic $Ttr::RFP^{Tg/+}$; $Afp::GFP^{Tg/+}$ embryos exhibit RFP fluorescence in both proximal and distal visceral endoderm, while GFP fluorescence is restricted to the distal visceral endoderm (l). By the MS (E6.5) stage, GFP fluorescence is gradually expanded into the proximal visceral endoderm (m). (**n**) At OB-LB stages (E7.5), RFP fluorescence is localized to the visceral endoderm overlying the extraembryonic ectoderm and a population of visceral endoderm-derived cells overlying the epiblast (white arrowhead). (**o,p**) By the 4 somite (o) and 6 somite (p) stages, RFP fluorescence is restricted to the extraembryonic visceral endoderm. (**q**) $Ttr::RFP^{Tg/+}$ embryo at 22 somite stage with RFP fluorescence in the visceral yolk sac. Pr, proximal; D, distal; A, anterior; P, posterior; 2D, 2-dimensions; 3D, 3-dimensions. Scale bars = 20 μm in f; 50 μm in j,l; 100 μm in g–i,k,m,n; 200 μm in o–q.

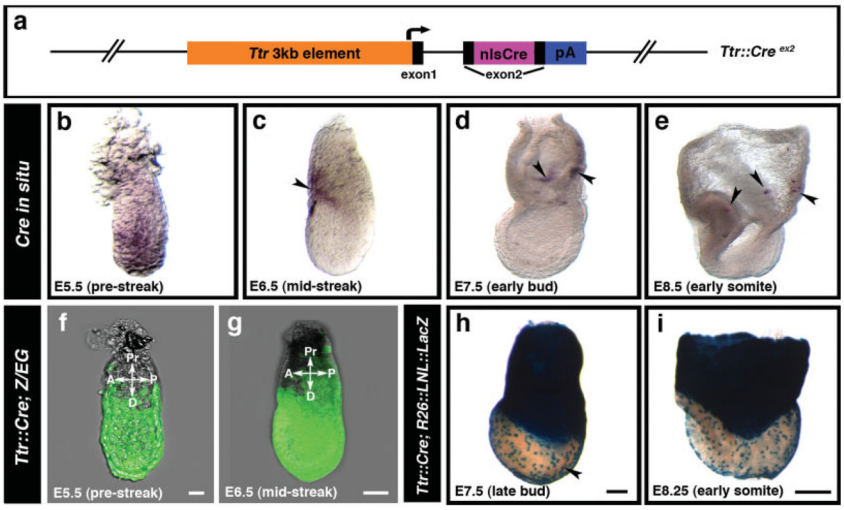

FIG. 2.

Cre-mediated recombination throughout the visceral endoderm in *Ttr::Cre* transgenics. (**a**) Schematic representation of the *Ttr::Cre* transgene containing an *nls*Cre insertion in the second exon. (**b–e**) Prestreak (E5.5) to early somite (E8.5) stage $Ttr::Cre^{Tg/+}$ embryos processed for *Cre* mRNA in situ hybridization. (**f,g**) The entire visceral endoderm at PS (E5.5) (f) and MS (E6.5) stages (g) in $Ttr::Cre^{Tg/+}$; $Z/EG^{Tg/+}$ embryos is labeled by Cre recombinase-mediated excision. (**h,i**) At LB (E7.5) (h) and ESom (E8.5) stages (i), the extraembryonic visceral endoderm and a population of visceral endoderm-derived cells overlying the epiblast (black arrowhead) is labeled in $Ttr::Cre^{Tg/+}$; $R26::LNL::LacZ^{+/-}$ embryos. Pr, proximal; D, distal; A, anterior; P, posterior. Scale bars = 20 μm in f; 50 μm in g; 100 μm in h; 200 μm in i.

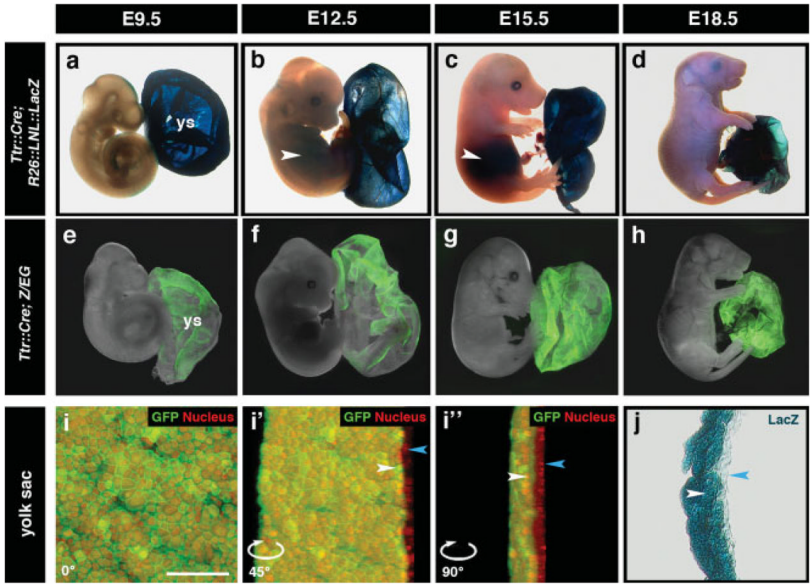

FIG. 3.

Cre-mediated recombination throughout the visceral yolk sac. (**a–d**) Wholemount view of mid- to late-gestational *Ttr::Cre*$^{Tg/+}$*; R26::LNL::LacZ*$^{+/-}$ embryos with labeling in the visceral yolk sac (blue stain) and liver (white arrowheads in b and c). (**e–h**) Wholemount view of mid- to late-gestational *Ttr::Cre*$^{Tg/+}$*; Z/EG*$^{Tg/+}$ embryos with GFP fluorescence in the visceral yolk sac. (i-i″) 3D reconstruction of yolk sac from an E12.5 *Ttr::Cre*$^{Tg/+}$*; Z/EG*$^{Tg/+}$ embryo (i) counterstained with Hoechst (labeling nuclei, red) and rotated 45 degrees (i′) and 90 degrees (i″). Green fluorescence is restricted to the yolk sac endoderm (white arrowheads) and excluded from the yolk sac mesoderm (blue arrowheads). (**j**) Transverse section through yolk sac of an E12.5 *Ttr::Cre*$^{Tg/+}$*; R26::LNL::LacZ*$^{+/-}$ embryo with LacZ staining in the yolk sac endoderm (white arrowhead) and no staining in the yolk sac mesoderm (blue arrowhead). Scale bars = 50 μm in i.

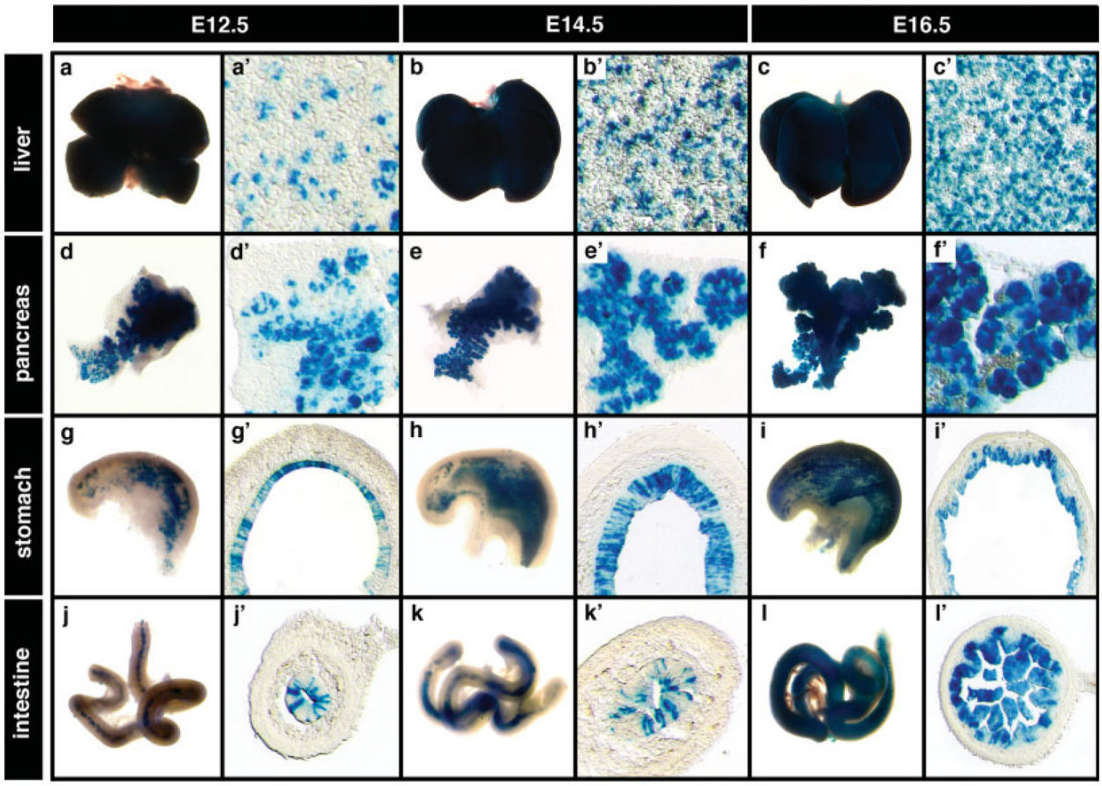

FIG. 4.

Cre-mediated recombination in various organs of mid- to late-gestational stages. (**a–l**) Wholemount views of organs from mid- to late-gestational *Ttr::Cre*$^{Tg/+}$*; R26::LNL::LacZ*$^{+/-}$ embryos with high β-gal activity in the liver (a–c), pancreas (d–f), stomach (g–i), and intestine (j–l). (**a′–c′**) Transverse sections through the liver show mosaic β-gal activity from E12.5 to E16.5. (**d′–f′**) In the pancreas, β-gal activity is restricted to the pancreatic epithelium and excluded from the pancreatic mesenchyme. (**g′–l′**) The epithelial lining of the stomach (g′–i′) and intestine (j′–l′) exhibit mosaic β-gal activity from E12.5 through E16.5.

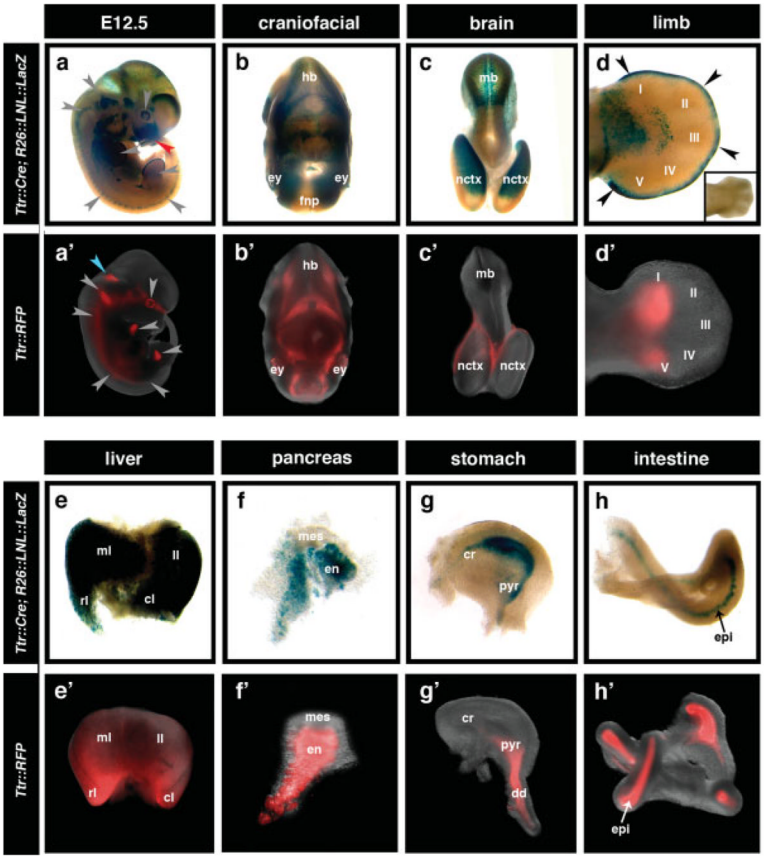

FIG. 5.

Additional sites of recombination in *Ttr::Cre* and expression in *Ttr::RFP* transgenics at later embryonic stages. (**a-a′**) Wholemount views depicting β-gal activity in *Ttr::Cre*$^{Tg/+}$; *R26::LNL::LacZ*$^{+/-}$ embryos (a) and RFP fluorescence in *Ttr::RFP* embryos (a′) at E12.5. Gray arrowheads highlight corresponding RFP fluorescence and Cre reporter activity in the optic vesicle, limb, trigeminal ganglion, and spinal ganglia; red arrowhead highlights Cre reporter activity in the frontal nasal process; blue arrowhead highlights RFP expression at the midbrain–hindbrain junction. (**b-b′**) *Cre* recombinase activity is closely correlated with RFP fluorescence in the craniofacial region with expression in the optic vesicle of the eye (ey) and hindbrain (hb). (**c-d′**) Cre reporter and RFP fluorescence are detected in the neocortex (nctx) of the brain (c-c′) and mesenchymal condensations in the limb (d-d′). In *Ttr::Cre*$^{Tg/+}$; *R26::LNL::LacZ*$^{+/-}$ embryos, the midbrain (mb) and apical ectodermal ridge (AER) also exhibits β-gal activity (black arrowheads in d), which is not detected endogenously in wild type control embryos (high magnification inset in d). (**e-h′**) Both *Ttr::Cre*$^{Tg/+}$; *R26::LNL::LacZ*$^{+/-}$ and *Ttr::RFP* embryos exhibit transgene expression in the fetal liver (e-e′), stomach (f-f′), pancreas (g-g′), and intestine (h-h′). ml, median lobe; rl, right lobe; ll, left lobe; cl, caudate lobe; mes, mesoderm; en, endoderm; cr, cardiac region; pyr, pyloric region; dd, duodenum; epi, epithelium.